Hindawi Publishing Corporation
EURASIP Journal on Advances in Signal Processing
Volume 2008, Article ID 672941, 13 pages
doi:10.1155/2008/672941

*Research Article*

# A Window Width Optimized S-Transform

**Ervin Sejdić,[1] Igor Djurović,[2] and Jin Jiang[1]**

[1] *Department of Electrical and Computer Engineering, The University of Western Ontario, London, Ontario, Canada N6A 5B9*
[2] *Electrical Engineering Department, University of Montenegro, 81000 Podgorica, Montenegro*

Correspondence should be addressed to Jin Jiang, jjiang@eng.uwo.ca

Received 14 May 2007; Accepted 15 November 2007

Recommended by Sven Nordholm

Energy concentration of the S-transform in the time-frequency domain has been addressed in this paper by optimizing the width of the window function used. A new scheme is developed and referred to as a window width optimized S-transform. Two optimization schemes have been proposed, one for a constant window width, the other for time-varying window width. The former is intended for signals with constant or slowly varying frequencies, while the latter can deal with signals with fast changing frequency components. The proposed scheme has been evaluated using a set of test signals. The results have indicated that the new scheme can provide much improved energy concentration in the time-frequency domain in comparison with the standard S-transform. It is also shown using the test signals that the proposed scheme can lead to higher energy concentration in comparison with other standard linear techniques, such as short-time Fourier transform and its adaptive forms. Finally, the method has been demonstrated on engine knock signal analysis to show its effectiveness.



## 1. INTRODUCTION

In the analysis of the nonstationary signals, one often needs to examine their time-varying spectral characteristics. Since time-frequency representations (TFR) indicate variations of the spectral characteristics of the signal as a function of time, they are ideally suited for nonstationary signals [1, 2]. The ideal time-frequency transform only provides information about the frequency occurring at a given time instant. In other words, it attempts to combine the local information of an instantaneous-frequency spectrum with the global information of the temporal behavior of the signal [3]. The main objectives of the various types of time-frequency analysis methods are to obtain time-varying spectrum functions with high resolution and to overcome potential interferences [4].

The S-transform can conceptually be viewed as a hybrid of short-time Fourier analysis and wavelet analysis. It employs variable window length. By using the Fourier kernel, it can preserve the phase information in the decomposition [5]. The frequency-dependent window function produces higher frequency resolution at lower frequencies, while at higher frequencies, sharper time localization can be achieved. In contrast to wavelet transform, the phase information provided by the S-transform is referenced to the time origin, and therefore provides supplementary information about spectra which is not available from locally referenced phase information obtained by the continuous wavelet transform [5]. For these reasons, the S-transform has already been considered in many fields such as geophysics [6–8], cardiovascular time-series analysis [9–11], signal processing for mechanical systems [12, 13], power system engineering [14], and pattern recognition [15].

Even though the S-transform is becoming a valuable tool for the analysis of signals in many applications, in some cases, it suffers from poor energy concentration in the time-frequency domain. Recently, attempts to improve the time-frequency representation of the S-transform have been reported in the literature. A generalized S-transform, proposed in [12], provides greater control of the window function, and the proposed algorithm also allows nonsymmetric windows to be used. Several window functions are considered, including two types of exponential functions: amplitude modulation and phase modulation by cosine functions. Another form of the generalized S-transform is developed in [7], where the window scale and shape are a function of frequency. The same authors introduced a bi-Gaussian window in [8], by joining two nonsymmetric half-Gaussian windows.

Since the bi-Gaussian window is asymmetrical, it also produces an asymmetry in the time-frequency representation, with higher-time resolution in the forward direction. As a result, the proposed form of the S-transform has better performance in detection of the onset of sudden events. However, in the current literature, none has considered optimizing the energy concentration in the time-frequency domain directly, that is, to minimize the spread of the energy beyond the actual signal components.

The main approach used in this paper is to optimize the width of the window used in the S-transform. The optimization is performed through the introduction of a new parameter in the transform. Therefore, the new technique is referred to as a window width optimized S-transform (WWOST). The newly introduced parameter controls the window width, and the optimal value can be determined in two ways. The first approach calculates one global, constant parameter and this is recommended for signals with constant or very slowly varying frequency components. The second approach calculates the time-varying parameter, and it is more suitable for signals with fast varying frequency components.

The proposed scheme has been tested using a set of synthetic signals and its performance is compared with the standard S-transform. The results have shown that the WWOST enhances the energy concentration. It is also shown that the WWOST produces the time-frequency representation with a higher concentration than other standard linear techniques, such as the short-time Fourier transform and its adaptive forms. The proposed technique is useful in many applications where enhanced energy concentration is desirable. As an illustrative example, the proposed algorithm is used to analyze knock pressure signals recorded from a Volkswagen Passat engine in order to determine the presence of several signal components.

This paper is organized as follows. In Section 2, the concept of ideal time-frequency transform is introduced, which can be compared with other time-frequency representations including transforms proposed here. The development of the WWOST is covered in Section 3. Section 4 evaluates the performance of the proposed scheme using test signals and also the knock pressure signals. Conclusions are drawn in Section 5.

## 2. ENERGY CONCENTRATION IN TIME-FREQUENCY DOMAIN

The ideal TFR should only be distributed along frequencies for the duration of signal components. Thus, the neighboring frequencies would not contain any energy; and the energy contribution of each component would not exceed its duration [3].

For example, let us consider two simple signals: an FM signal, $x_1(t) = A(t)\exp(j\phi(t))$, where $|dA(t)/dt| \ll |d\phi(t)/dt|$ and the instantaneous frequency is defined as $f(t) = (d\phi(t)/dt)/2\pi$; and a signal with the Fourier transform given as $X(f) = G(f)\exp(j2\pi\chi(f))$, where the spectrum is slowly varying in comparison to phase $|dG(f)/df| \ll |d\chi(f)/df|$. Further, $A(t)$ and $G(t)$ The ideal TFRs for these signals are given, respectively, as shown in [16]

$$\mathrm{ITFR}(t,f) = 2\pi A(t)\delta\left(f - \frac{1}{2\pi}\frac{d\phi(t)}{dt}\right), \tag{1}$$

$$\mathrm{ITFR}(t,f) = 2\pi G(f)\delta\left(t + \frac{d\chi(f)}{df}\right), \tag{2}$$

where ITFR stands for an ideal time-frequency representation. These two representations are ideally concentrated along the instantaneous frequency, $(d\phi(t)/dt)/2\pi$, and on group delay $-d\chi(f)/df$. Simplest examples of these signals are the following: a sinusoid with $A = \text{const.}$ and $d\phi(t)/dt = \text{const.}$ depicted in Figure 1(a); and a Dirac pulse $x_2(t) = \delta(t - t_0)$ shown in Figure 1(b). The ideal time-frequency representations are depicted in Figures 1(c) and 1(d). These two graphs are compared with the TFRs obtained by the standard S-transform in Figures 1(e) and 1(f).

For the sinusoidal case, the frequencies surrounding $(d\phi(t)/dt)/2\pi$ also have a strong contribution, and from (1), it is clear that they should not have any contributions. Similarly, for the Dirac function, it is expected that all the frequencies have the contribution but only for a single time instant. Nevertheless, it is clear that the frequencies are not only contributing during a single time instant as expected from (2), but the surrounding time instants also have strong energy contribution.

The examples presented here are for illustrations only, since a priori knowledge about the signals is assumed. In most practical situations, the knowledge about a signal is limited and the analytical expressions similar to (1) and (2) are often not available. However, the examples illustrate a point that some modifications to the existing S-transform algorithm, which do not assume a *priori* knowledge about the signal, may be useful to achieve improved performance in time-frequency energy concentration. Such improvements only become possible after modifications to the width of the window function are made.

## 3. THE PROPOSED SCHEME

### 3.1. Standard S-transform

The standard S-transform of a function $x(t)$ is given by an integral as in [5, 7, 12]

$$S_x(t,f) = \int_{-\infty}^{+\infty} x(\tau)w(t-\tau,\sigma(f))\exp(-j2\pi f\tau)d\tau \tag{3}$$

with a constraint

$$\int_{-\infty}^{+\infty} w(t-\tau,\sigma(f))d\tau = 1. \tag{4}$$

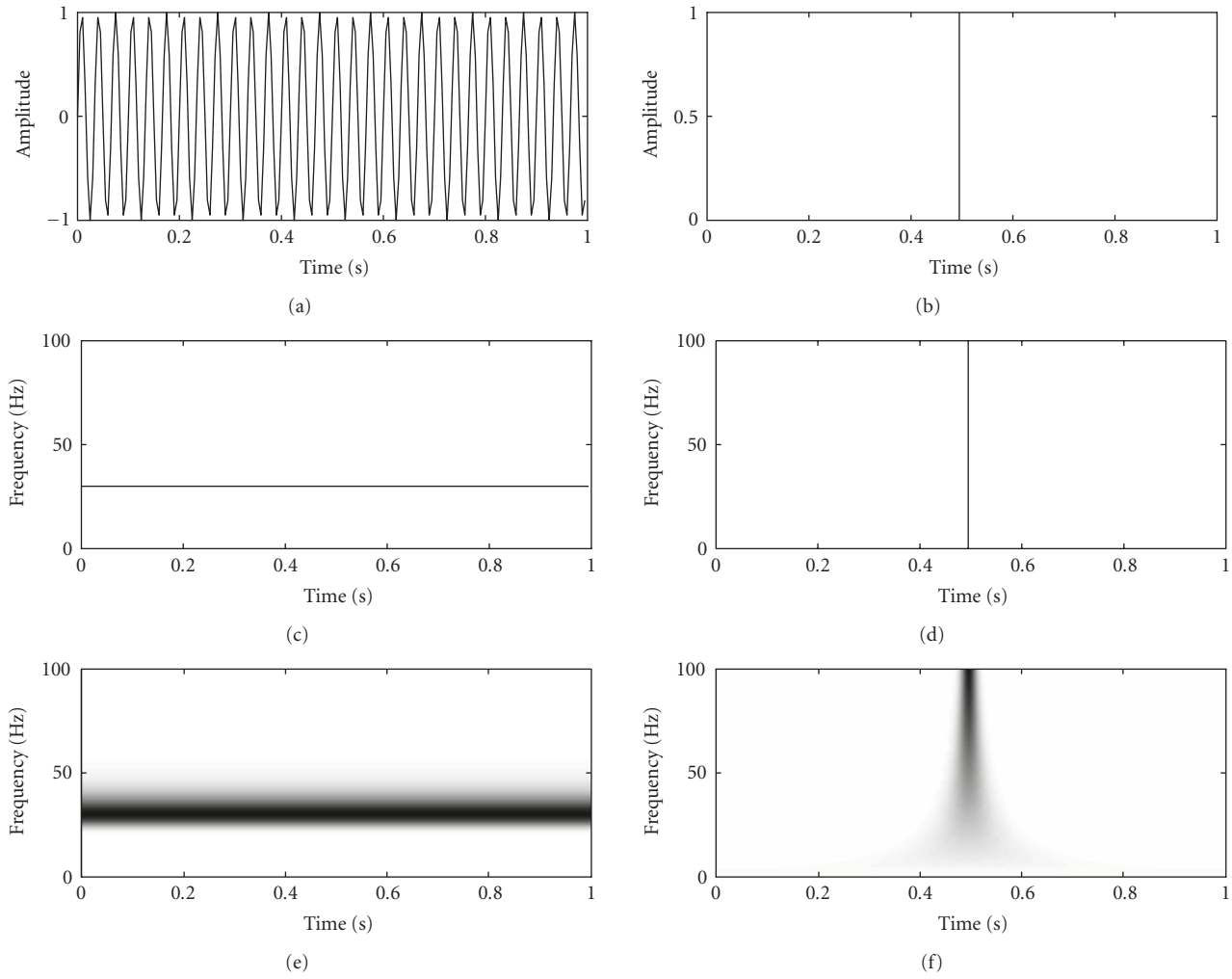


Figure 1: Comparison of the ideal time-frequency representation and S-transform for the two simple signal forms: (a) 30 Hz sinusoid; (b) sample Dirac function; (c) ideal TFR of a 30 Hz sinusoid; (d) ideal TFR of a Dirac function; (e) TFR by standard S-transform for a 30 Hz sinusoid; and (f) TFR by standard S-transform of the Dirac delta function.

A window function used in S-transform is a scalable Gaussian function defined as

$$w(t, \sigma(f)) = \frac{1}{\sigma(f)\sqrt{2\pi}} \exp\left( -\frac{t^2}{2\sigma^2(f)} \right). \tag{5}$$

The advantage of the S-transform over the short-time Fourier transform (STFT) is that the standard deviation $\sigma(f)$ is actually a function of frequency, $f$, defined as

$$\sigma(f) = \frac{1}{|f|}. \tag{6}$$

Consequently, the window function is also a function of time and frequency. As the width of the window is dictated by the frequency, it can easily be seen that the window is wider in the time domain at lower frequencies, and narrower at higher frequencies. In other words, the window provides good localization in the frequency domain for low frequencies while providing good localization in time domain for higher frequencies.

The disadvantage of the current algorithm is the fact that the window width is always defined as a reciprocal of the frequency. Some signals would benefit from different window widths. For example, for a signal containing a single sinusoid, the time-frequency localization can be considerably improved if the window is very narrow in the frequency domain. Similarly, for signals containing only a Dirac impulse, it would be beneficial for good time-frequency localization to have very wide window in the frequency domain.

### 3.2. Window width optimized S-transform

A simple improvement to the existing algorithm for the S-transform can be made by modifying the standard deviation of the window to

$$\sigma(f) = \frac{1}{|f|^p}. \tag{7}$$

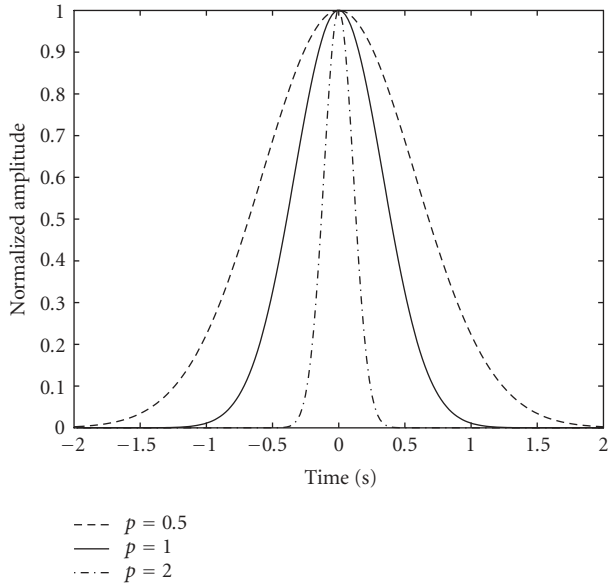


Figure 2: Normalized Gaussian window for different values of $p$.

Based on the above equation, the new S-transform can be represented as

$$S_x^p(t,f) = \frac{|f|^p}{\sqrt{2\pi}} \int_{-\infty}^{+\infty} x(\tau) \exp\left(-\frac{(t-\tau)^2 f^{2p}}{2}\right) \exp(-j2\pi f\tau) d\tau. \tag{8}$$

The parameter $p$ can control the width of the window. By finding an appropriate value of $p$, an improved time-frequency concentration can be obtained. The window functions with three different values of $p$ are plotted in Figure 2, where $p = 1$ corresponds to the standard S-transform window. For $p < 1$, the window becomes wider in the time domain, and for $p > 1$, the window narrows in the time domain. Therefore, by considering the example from Section 2, for the single sinusoid, a small value of $p$ would provide almost perfect concentration of the signal, whereas for the Dirac function, a rather large value of $p$ would produce a good concentration in the time-frequency domain. It is important to mention that in the case of $0 < f < 1$, the opposite is true.

The optimal value of $p$ will be found based on the concentration measure proposed in [17], which has some favorable performance in comparison to other concentration measures reported in [18–20]. The measure is designed to minimize the energy concentration for any time-frequency representation based on the automatic determination of some time-frequency distribution parameter. This measure is defined as

$$\mathrm{CM}(p) = \frac{1}{\int_{-\infty}^{+\infty}\int_{-\infty}^{+\infty} |S_x^p(t,f)|\, dt\, df}, \tag{9}$$

where CM stands for a concentration measure.

There are two ways to determine the optimal value of $p$. One is to determine a global, constant value of $p$ for the entire signal. The other is to determine a time-varying $p(t)$, which depends on each time instant considered. The first approach is more suitable for signals with the constant or slowly varying frequency components. In this case, one value of $p$ will suffice to give the best resolution for all components. The time-varying parameter is more appropriate for signals with fast varying frequency components. In these situations, depending on the time duration of the signal components, it would be beneficial to use lower value of $p$ (somewhere in the middle of the particular component's interval), and to use higher values of $p$ for the beginning and the end of the component's interval, so the component is not smeared in the time-frequency plane. It is important to mention that both proposed schemes for determining the parameter $p$ are the special cases of the algorithm which would evaluate the parameter on any arbitrary subinterval, rather than over the entire duration of the signal.

#### 3.2.1. Algorithm for determining the time-invariant $p$

The algorithm for determining the optimized time-invariant value of $p$ is defined through the following steps.

(1) For $p$ selected from a set $0 < p \leq 1$, compute S-transform of the signal $S_x^p(t,f)$ using (8).

(2) For each $p$ from the given set, normalize the energy of the S-transform representation, so that all of the representations have the equal energy

$$\overline{S_x^p(t,f)} = \frac{S_x^p(t,f)}{\sqrt{\int_{-\infty}^{+\infty}\int_{-\infty}^{+\infty} |S_x^p(t,f)|^2\, dt\, df}}. \tag{10}$$

(3) For each $p$ from the given set, compute the concentration measure according to (9), that is,

$$\mathrm{CM}(p) = \frac{1}{\int_{-\infty}^{+\infty}\int_{-\infty}^{+\infty} |\overline{S_x^p(t,f)}|\, dt\, df}. \tag{11}$$

(4) Determine the optimal parameter $p_{\mathrm{opt}}$ by

$$p_{\mathrm{opt}} = \max_p [\mathrm{CM}(p)]. \tag{12}$$

(5) Select $S_x^p(t,f)$ with $p_{\mathrm{opt}}$ to be the WWOST

$$S_x^p(t,f) = S_x^{p_{\mathrm{opt}}}(t,f). \tag{13}$$

As it can be seen, the proposed algorithm computes the S-transform for each value of $p$ and, based on the computed representation, it determines the concentration measure, $\mathrm{CM}(p)$, as an inverse of $L^1$ norm of the normalized S-transform for a given $p$. The maximum of the concentration measure corresponds to the optimal $p$ which provides the least smear of $\overline{S_x^p(t,f)}$.

It is important to note that in the first step, the value of $p$ is limited to the range $0 < p \leq 1$. Any negative value of $p$ corresponds to an $n$th root of a frequency which would make the window wider as frequency increases. Similarly, values

greater than 1 provide a window which may be too narrow in the time domain. Unless the signal being analyzed is a superposition of Delta functions, the value of $p$ should not exceed unity. As a special case, it is important to point out that for $p = 0$, the WWOST is equivalent to STFT with a Gaussian window with $\sigma^2 = 1$.

#### 3.2.2. Algorithm for determining $p(t)$

The time-varying parameter $p(t)$ is required for signals with components having greater or abrupt changes. The algorithm for choosing the optimal $p(t)$ can be summarized through the following steps.

(1) For $p$ selected from a set $0 < p(t) \leq 1$, compute S-transform of the signal $S_x^p(t, f)$ using (8).

(2) Calculate the energy, $E_1$, for $p = 1$. For each $p$ from the set, normalize the energy of the S-transform representation to $E_1$, so that all of the representations have the equal energy, and the amplitude of the components is not distorted,

$$\overline{S_x^p(t,f)} = \sqrt{E_1}\frac{S_x^p(t,f)}{\sqrt{\int_{-\infty}^{+\infty}\int_{-\infty}^{+\infty}\left|S_x^p(t,f)\right|^2 dt\,df}}. \tag{14}$$

(3) For each $p$ from the set and a time instant $t$, compute

$$\mathrm{CM}(t,p) = \frac{1}{\int_{-\infty}^{+\infty}\left|\overline{S_x^p(t,f)}\right| df}. \tag{15}$$

(4) Optimal value of $p$ for the considered instant $t$ maximizes concentration measure $\mathrm{CM}(t, p)$,

$$p_{\mathrm{opt}}(t) = \arg\max_p \left[\mathrm{CM}(t,p)\right]. \tag{16}$$

(5) Set the WWOST to be

$$S_x^p(t,f) = S_x^{p_{\mathrm{opt}}(t)}(t,f). \tag{17}$$

The main difference between the two techniques lies in step (3). For the time invariant case, a single value of $p$ is chosen, whereas in the time-varying case, an optimal value of $p(t)$ is a function of time. As it is demonstrated in Section 4, the time-dependent parameter is beneficial for signals with the fast varying components.

#### 3.2.3. Inverse of the WWOST

Similarly to the standard S-transform, the WWOST can be used as both an analysis and a synthesis tool. The inversion procedure for the WWOST resembles that of the standard S-transform, but with one additional constraint. The spectrum of the signal obtained by averaging $S_x^p(t, f)$ over time must be normalized by $W(0, f)$, where $W(\alpha, f)$ represents the Fourier transform (from $t$ to $\alpha$) of the window function, $w(t, \sigma(f))$. Hence, the inverse WWOST for a signal, $x(t)$, is defined as

$$x(t) = \int_{-\infty}^{+\infty}\int_{-\infty}^{+\infty}\frac{1}{W(0,f)}S_x^p(\tau,f)\exp\left(j2\pi f t\right)d\tau\,df. \tag{18}$$

In the case of a time-invariant $p$, it can be shown that $W(0, f) = 1$. In a general case, the Fourier transform of the proposed modified window can only be determined numerically.

## 4. WWOST PERFORMANCE ANALYSIS

In this section, the performance of the proposed scheme is examined using a set of synthetic test signals first. Furthermore, the analysis of signals from an engine is also given. The first part includes two cases: (1) a simple case involving three slowly varying frequencies and (2) more complicated cases involving multiple time-varying components. The goal is to examine the performance of WWOST in comparison to the standard S-transform. The proposed algorithm is also compared to other time-frequency representations, such as the short-time Fourier transform (STFT) and adaptive STFT (ASTFT), to highlight the improved performance of the S-transform with the proposed window width optimization technique. In particular, the proposed algorithm can be used for some classes of the signals for which the standard S-transform would not be suitable.

As for the synthetic signals, the sampling period used in the simulations is $T_s = 1/256$ seconds. Also, the set of $p$ values, used in the numerical analysis of both test and the knock pressure signals, is given by $p = \{0.01n : n \in \mathbb{N} \text{ and } 1 \leq n \leq 100\}$. The ASTFT is calculated according to the concentration measure given by (9). In the definition of the measure, a normalized STFT is used instead of the normalized WWOST. The standard deviation of the Gaussian window, $\sigma_{\mathrm{gw}}$, is used as the optimizing parameter, where the window is defined as

$$w_{\mathrm{STFT}}(t) = \frac{1}{\sigma_{\mathrm{gw}}\sqrt{2\pi}}\exp\left(-\frac{t^2}{2\sigma_{\mathrm{gw}}^2}\right). \tag{19}$$

The optimization for synthetic signals is performed on the set of values defined by

$$\sigma_{\mathrm{gw}} = \{n/128 : n \in \mathbb{N},\ 1 \leq n \leq 128\} \tag{20}$$

and both the time-invariant and time-varying values of $\sigma_{\mathrm{gw}}$ are calculated.

### 4.1. Synthetic test signals

*Example 1.* The first test signal is shown in Figure 3(a). It has the following analytical expression:

$$\begin{aligned} x_1(t) = {} & \cos\left(132\pi t + 14\pi t^2\right) + \cos\left(10\pi t - 2\pi t^2\right) \\ & + \cos\left(30\pi t + 6\pi t^2\right), \end{aligned} \tag{21}$$

where the signal exists only on the interval $0 \leq t < 1$. The signal consists of three slowly varying frequency components. It is analyzed using the STFT (Figure 3(b)), ASTFT with time-invariant optimum value of $\sigma_{\mathrm{gw}}$ (Figure 3(c)), standard S-transform (Figure 3(d)), and the proposed algorithm (Figure 3(f)). A Gaussian window is also used in the analysis by the STFT, with standard deviations equal to 0.05. The

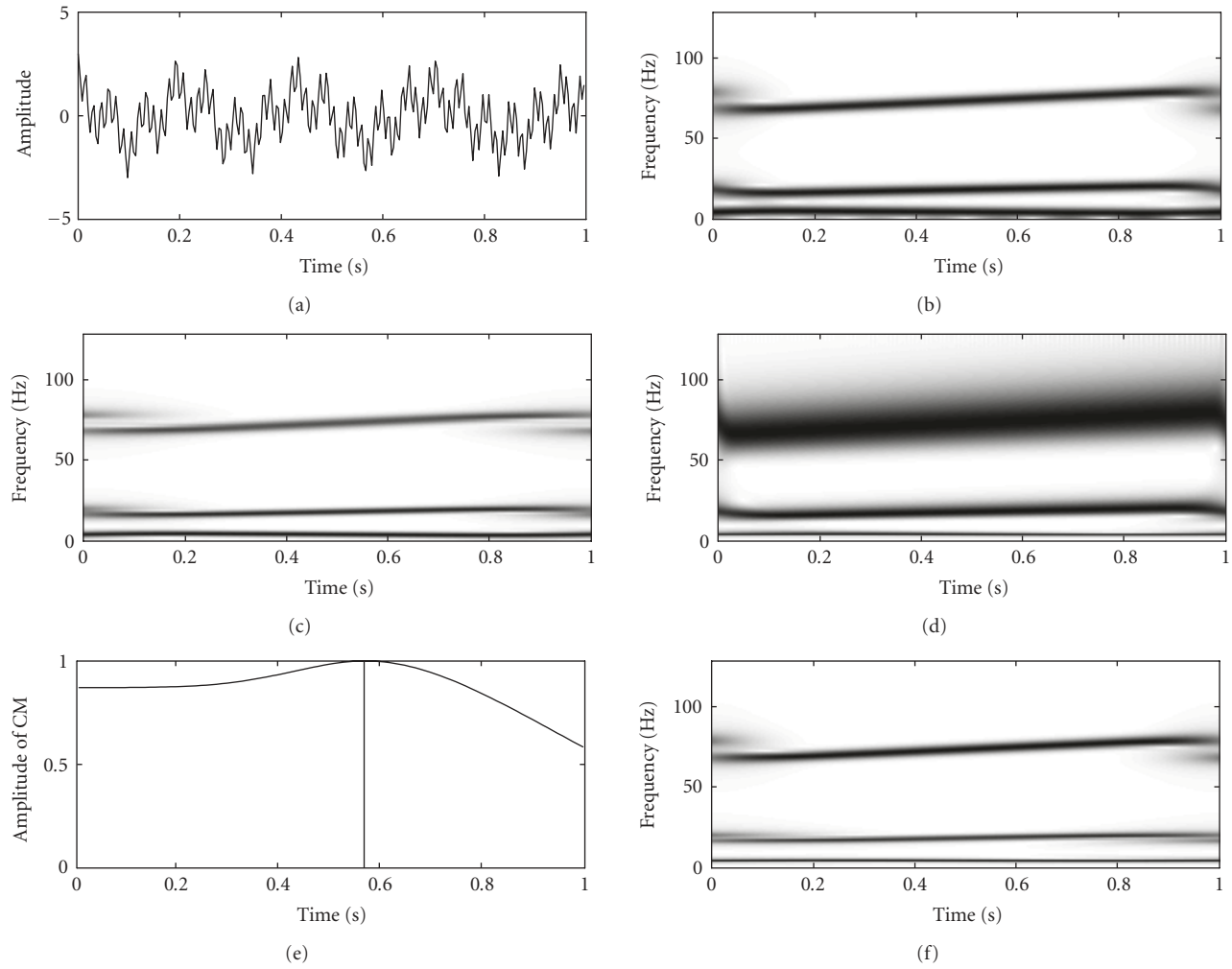


Figure 3: Test signal $x_1(t)$: (a) time-domain representation; (b) STFT of $x_1(t)$; (c) ASTFT of $x_1(t)$ with $\sigma_{\text{opt}}$; (d) $S_x^p(t, f)$ of $x_1(t)$ with $p = 1$ (standard S-transform); (e) concentration measure CM($p$); (f) $S_x^p(t, f)$ of $x_1(t)$ with the optimal value of $p = .57$.

optimum value of standard deviation for the ASTFT is calculated to be $\sigma_{\text{opt}} = 0.094$. The colormap used for plotting the time-frequency representations in Figure 3 and all the subsequent figures is a linear grayscale with values from 0 to 1.

The standard S-transform, shown in Figure 3(d), depicts all three components clearly. However, only the first two components have relatively good concentration, while the third component is completely smeared in frequency. As shown in Figure 3(b), the STFT provides better energy concentration than the standard S-transform. The ASTFT, depicted in Figure 3(c), shows a noticeable improvement for all three components. The results with the proposed scheme is shown in Figure 3(f) for $p = 0.57$. The value of $p$ is found according to (12). For the determined value of $p$, the first two components have higher concentration even than the ASTFT, while the third component has approximately the same concentration.

In Figure 3(e), the normalized concentration measure is depicted. The obtained results verify the theoretical predictions from Section 3.2. For this class of signals, that is, the signals with slowly varying frequencies, it is expected that smaller values of $p$ will produce the best energy concentration. In this example, the optimal value, found according to (12), is determined numerically to be 0.57.

Based on the visual inspection of the time-frequency representations shown in Figure 3, it can be concluded that the proposed algorithm achieves higher concentration among the considered representations. To confirm this fact, a performance measure given by

$$\Xi_{\text{TF}} = \left( \int_{-\infty}^{+\infty} \int_{-\infty}^{+\infty} |\overline{\text{TF}(t, f)}|\, dt\, df \right)^{-1} \tag{22}$$

is used for measuring the concentration of the representation, where $|\overline{\text{TF}(t, f)}|$ is a normalized time-frequency representation. The performance measure is actually the concentration measure proposed in (9). A more concentrated representation will produce a higher value of $\Xi_{\text{TF}}$. Table 1 summarizes the performance measure for the STFT, the ASTFT, the standard S-transform, and the WWOST.

Table 1: Performance measure for the three time-frequency transforms.

| TFR | $\Xi_{TF}$ |
|---|---|
| STFT | 0.0119 |
| ASTFT | 0.0131 |
| Standard S-transform | 0.0080 |
| WWOST | 0.0136 |

The value of the performance measure for the standard S-transform is the lowest, followed by the STFT. The WWOST produces the highest value of $\Xi_{TF}$, and thus achieves a TFR with the highest energy concentration amongst the transforms considered.

*Example 2.* The signal in the second example contains multiple components with faster time-varying spectral contents. The following signal is used:

$$x_2(t) = \cos\big[40\pi(t-0.5)\arctan(21t-10.5) - 20\pi\ln\left((21t-10.5)^2+1\right)/21 + 120\pi t\big] + \cos\left(40\pi t - 8\pi t^2\right), \quad (23)$$

where $x_2(t)$ exists only on the interval $0 \le t < 1$. This signal consists of two components. The first has a transition region from lower to higher frequencies, and the second is a linear chirp. In the analysis, the time-frequency transformations that employ a constant window exhibit a conflicting issue between good concentration of the transition region for the first component versus good concentration for the rest of the signal. In order to numerically demonstrate this problem, the signal is again analyzed using the STFT (Figure 4(a)), ASTFT with the optimal time-invariant value of $\sigma_{gw}$ (Figure 4(c)), ASTFT with the optimal time-varying value of $\sigma_{gw}$ (Figure 4(e)), standard S-transform (Figure 4(b)), the proposed algorithm with both time-invariant (Figure 4(d)), and time-varying $p$ (Figure 4(f)). A Gaussian window is used for the STFT, with $\sigma = 0.03$. The optimum time-invariant value of the standard deviation for the ASTFT is determined to be $\sigma_{opt} = 0.055$.

The standard deviation of the Gaussian window used should be small in order for the STFT to provide relatively good concentration in the transition region. However, as the value of the standard deviation decreases, so is the concentration of the rest of the signal. To a certain extent, the standard S-transform is capable of producing a good concentration around the instantaneous frequencies at the lower frequencies and also in the transition region for the first component. However, at the high frequencies, the standard S-transform exhibits poor concentration for the first component. The WWOST with a time-invariant $p$ enhances the concentration of the linear chirp, as shown in Figure 4(d). However the concentration of the transition region of the first component has deteriorated in comparison to the standard S-transform. The concentration obtained with the WWOST with the time-invariant $p$ for this transition region is equivalent to the poor concentration exhibited by the STFT. Even though the ASTFT with both time-invariant and time-varying optimum values of standard deviation provide good concentration of the linear FM component and the stationary parts of the second component, the transition region of the second component is smeared in time.

Table 2: Performance measures for the time-frequency representations considered in Example 2.

| TFR | $\Xi_{TF}$ |
|---|---|
| STFT | 0.0108 |
| ASTFT with $\sigma_{opt}$ | 0.0115 |
| ASTFT with $\sigma_{opt}(t)$ | 0.0119 |
| WWOST with $p$ | 0.0116 |
| WWOST with $p(t)$ | 0.0124 |

Figure 4(f) represents the signal optimized S-transform obtained by using $p(t)$. A significant improvement in the energy concentration is easily noticeable in comparison to the standard S-transform. All components show improved energy concentration in comparison to the S-transform. Further, a comparison of the representations obtained by the proposed implementation of the S-transform and the STFT shows that both components have higher energy concentration in the representation obtained by the WWOST with $p(t)$.

As mentioned previously, for this type of signals it is more appropriate to use the time-varying $p(t)$ rather than a single constant $p$ value in order to achieve better concentration of the nonstationary data. By comparing Figures 4(d) and 4(f), the component with the fast changing frequency has better concentration with $p(t)$ than a fixed $p$, which is calculated according to (12), while the linear chirp has similar concentration in both cases.

It would be beneficial to quantify the results by evaluating the performance measure again. The performance measure is given by (22) and the results are summarized in Table 2. A higher value of the performance measure for WWOST with $p(t)$ reconfirms that the time-varying algorithm should be used for the signals with fast changing components. Also, it is worthwhile to examine the value of (22) for the STFT and the ASTFT. The time-frequency representations of the signal obtained by the STFT and ASTFT algorithms achieve smaller values of the performance measure than WWOST. This supports the earlier conclusion that the WWOST produces more concentrated energy representation than the STFT and ASTFT. The WWOST with the time-invariant value of $p$ produces higher concentration than the ASTFT with the optimum time-invariant value of $\sigma_{gw}$, and the WWOST with $p(t)$ produces higher concentration than the ASTFT with the optimum time-varying value of the $\sigma_{gw}$.

*Example 3.* Another important class of signals are those with crossing components that have fast frequency variations. A representative signal as shown in Figure 5(a) is given by

$$x_3(t) = \cos\left(20\pi\ln(10t+1)\right) + \cos\left(48\pi t + 8\pi t^2\right) \quad (24)$$

with $x_3(t) = 0$ outside the interval $0 \le t < 1$. For this class of signals, similar conflicting issues occur as in the

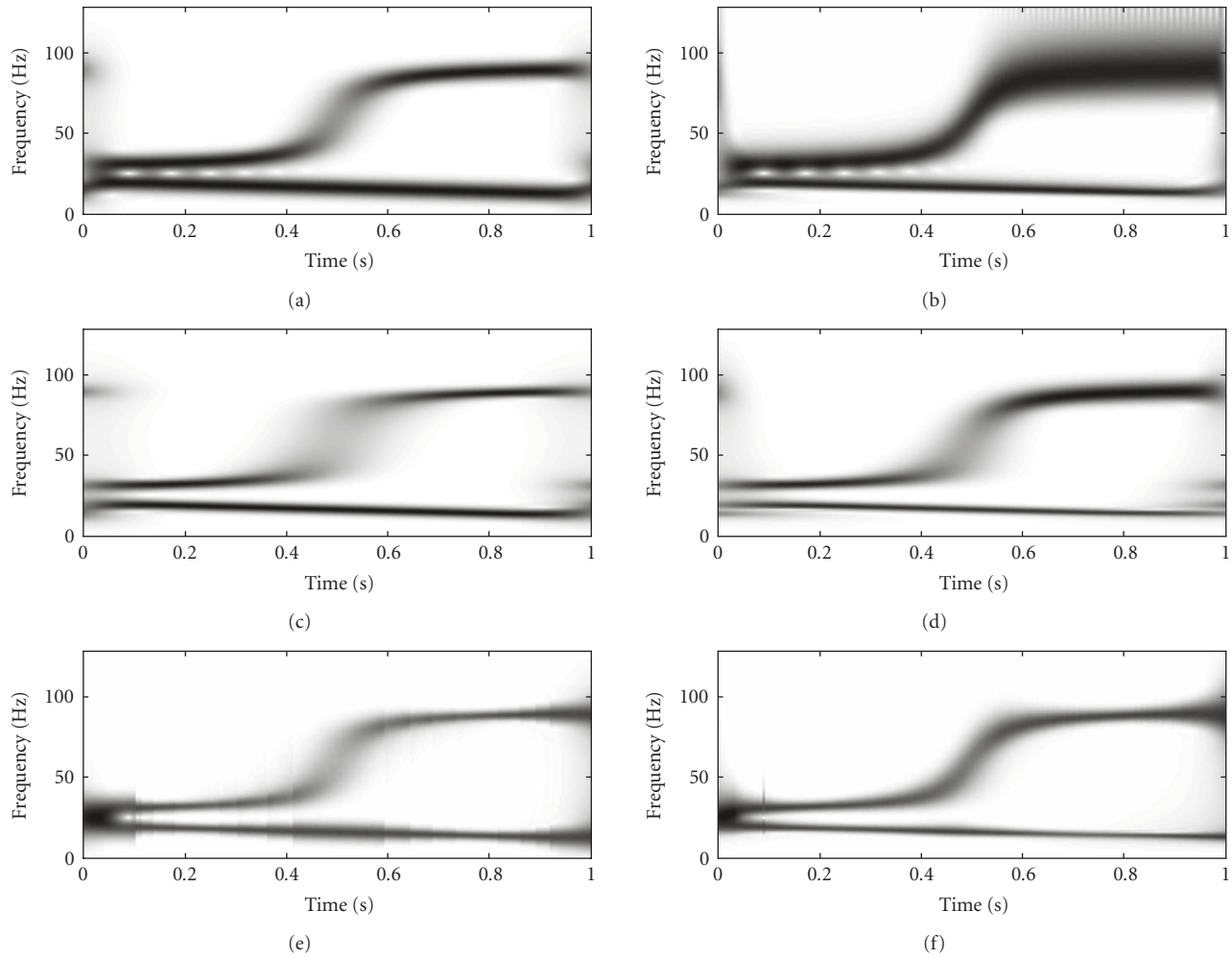


Figure 4: Comparison of different algorithms: (a) STFT of $x_2(t)$; (b) $S_x^p(t, f)$ of $x_2(t)$ with $p = 1$ (standard S-transform); (c) ASTFT of $x_2(t)$ with $\sigma_{\text{opt}} = 0.055$; (d) $S_x^p(t, f)$ of $x_2(t)$ with $p = 0.73$; (e) ASTFT of $x_2(t)$ with $\sigma_{\text{opt}}(t)$; (f) $S_x^p(t, f)$ of $x_2(t)$ with the optimal $p(t)$.

previous example; however, here exists an additional constraint, that is, the crossing components. The time-frequency analysis is performed using the STFT (Figure 5(b)), the ASTFT with the time-varying $\sigma_{\text{gw}}$ (Figure 5(c)), the standard S-transform (Figure 5(d)), and the proposed algorithm for the S-transform (Figure 5(f)). In the STFT, a Gaussian window with a standard deviation of 0.02 is used. Due to the time-varying nature of the frequency components present in the signal, the time-varying algorithm is used in the calculation of the WWOST in order to determine the optimal value of $p$.

The representation obtained by the STFT depicts good concentration of the higher frequencies, while having relatively poor concentration at the lower frequencies. An improvement in the concentration of the lower frequencies is obtained with the ASTFT algorithm. The standard S-transform is capable of providing better concentration for the high frequencies, but for the linear chirp, the concentration is equivalent to that of the STFT.

From the time-frequency representation obtained by the WWOST, it is clear that the concentration is preserved at high frequencies, while the linear chirp has significantly higher concentration in comparison to the other representations. It is also interesting to note how $p(t)$ varies between 0.6 and 1.0 as a function of time shown in Figure 5(e). In particular, $p(t)$ is close to 1 at the beginning of the signal in order to achieve good concentration of the high-frequency component. As time progresses, the value of $p(t)$ decreases in order to provide a good concentration at the lower frequencies. Towards the end of the signal, $p(t)$ increases again to achieve a good time localization of the signal.

In Section 3, it has been stated that for the components with faster variations, it is recommended that the time-varying algorithm with the WWOST be used. In order to substantiate that statement, the performance measure implemented in the previous examples is used again and the results are shown in Table 3. The optimized time-invariant value of the parameter $p_{\text{opt}}$ for this signal, found according to (12), is determined numerically to be 0.71. These performance measures verify that the time-varying algorithm should be used for the faster varying components. For comparison purposes, the performance measures for the representations given by

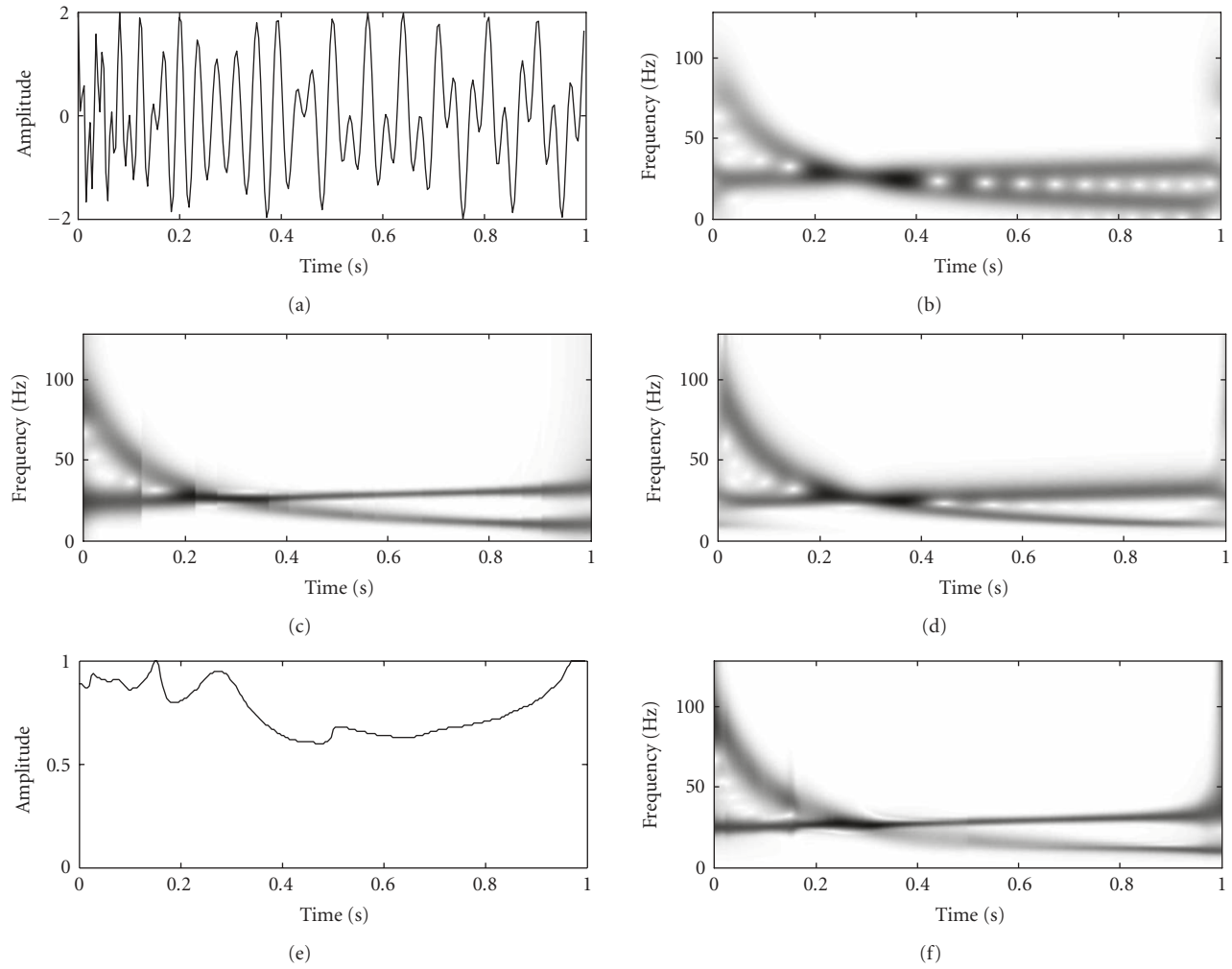


Figure 5: Time-frequency analysis of signal with fast variations in frequency: (a) time-domain representation; (b) STFT of $x_3(t)$; (c) ASTFT of $x_3(t)$ with $\sigma_{\text{opt}}(t)$; (d) $S_x^p(t, f)$ of $x_3(t)$ with $p = 1$ (standard S-transform); (e) $p(t)$; (f) $S_x^p(t, f)$ of $x_3(t)$ with the optimal $p(t)$.

Table 3: Performance measures for the time-frequency representations considered in Example 3.

| TFR | $\Xi_{\text{TF}}$ (noise-free) | $\Xi_{\text{TF}}$ (SNR = 25 dB) |
|---|---|---|
| STFT | 0.0106 | 0.0100 |
| ASTFT with $\sigma_{\text{opt}}$ | 0.0121 | 0.0114 |
| ASTFT with $\sigma_{\text{opt}}(t)$ | 0.0122 | 0.0113 |
| WWOST with $p$ | 0.0122 | 0.0110 |
| WWOST with $p(t)$ | 0.0126 | 0.0116 |

the STFT and its time-invariant ($\sigma_{\text{opt}} = 0.048$) and time-varying adaptive algorithms are calculated as well. By comparing the values of the performance measure for different time-frequency transforms, these values confirm the earlier statement which assures that each algorithm for the WWOST produces more concentrated time-frequency representation in its respective class than the ASTFT.

In the analysis performed so far, it was assumed that the signal-to-noise ratio (SNR) is infinity, that is, the noise-free signals were considered. It would be beneficial to compare the performance of the considered algorithms in the presence of additive white Gaussian noise in order to understand whether the proposed algorithm is capable of providing the enhanced performance in noisy environment. Hence, the signal $x_3(t)$ is contaminated with the additive white Gaussian noise and it is assumed that SNR = 25 dB. The results of such an analysis are summarized in Table 3. Even though, the performance has degraded in comparison to the noiseless case, the WWOST with $p(t)$ still outperforms the other considered representations.

### 4.2. Demonstration example

In order to illustrate the effectiveness of the proposed scheme, the method has been applied to the analysis of engine knocks. A knock is an undesired spontaneous autoignition of the unburned air-gas mixture causing a rapid increase in pressure and temperature. This can lead to serious problems in spark-ignition car engines, for example,

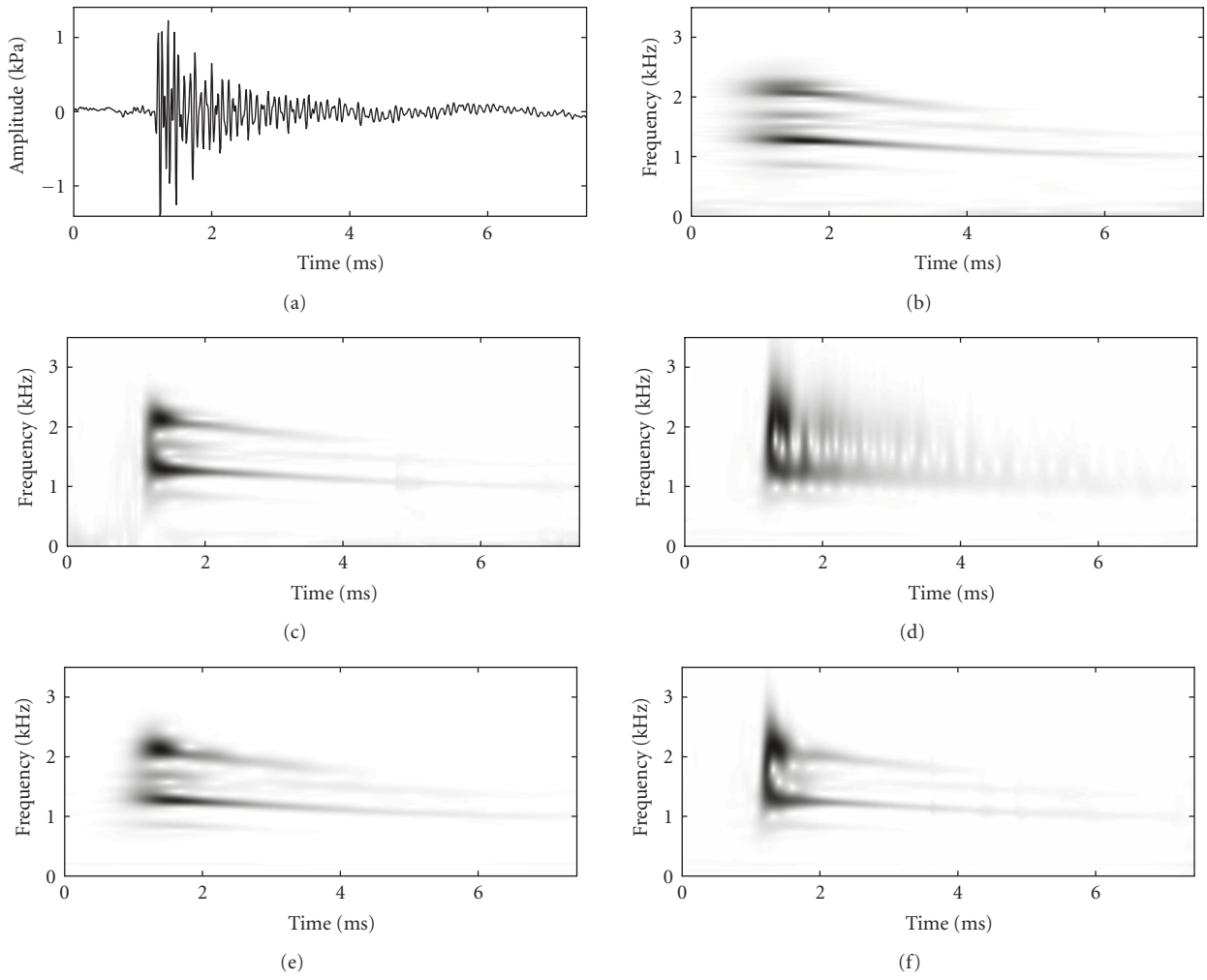


Figure 6: Time-frequency analysis of engine knock pressure signal (17th trial): (a) time-domain representation; (b) STFT; (c) ASTFT with $\sigma_{\text{opt}}(t)$; (d) $S_x^p(t, f)$ with $p = 1$ (standard S-transform); (e) $S_x^p(t, f)$ with $p = 0.86$; (f) $S_x^p(t, f)$ with the optimal $p(t)$.

environment pollution, mechanical damages, and reduced energy efficiency [21, 22]. In this paper, a focus will be on the analysis of knock pressure signals.

It has been previously shown that high-pass filtered pressure signals in the presence of knocks can be modeled as multicomponent FM signals [22]. Therefore, the goal of this analysis is to illustrate how effectively the proposed WWOST can decouple these components in time-frequency representation. A knock pressure signal recorded from a 1.81 Volkswagen Passat engine at 1200 rpm is considered. Note that the signal is high-pass filtered with a cutoff frequency of 3000 Hz. The sampling rate is $f_s = 100$ kHz and the signal contains 744 samples.

The performance of the proposed scheme in this case is evaluated by comparing it with that of the STFT, the ASTFT, and the standard S-transform. The results are shown in Figures 6 and 7. These results represent two sample cases from fifty trials. For the STFT, a Gaussian window, with a standard deviation of 0.3 milliseconds, is used for both cases. The optimization of the standard deviation for the ASTFT is performed on the set of values defined by $\sigma_{\text{gw}} = \{0.01n : n \in \mathbb{N} \text{ and } 1 \leq n \leq 744\}$ milliseconds.

A comparison of these representations show that the WWOST performs significantly better than the standard S-transform. The presence of several signal components can be easily identified with the WWOST, but rather difficult with the standard S-transform. In addition, both proposed algorithms produce higher concentration than the STFT and the corresponding class of the ASTFT. This is accurately depicted through the results presented in Table 4. The best concentration is achieved with the time-varying algorithm, while the time invariant value $p$ produces slightly higher concentration than the ASTFT with the time-invariant value of $\sigma_{\text{gw}}$ ($\sigma_{\text{opt}} = 0.2$ milliseconds for the signal in Figure 6 and $\sigma_{\text{opt}} = 0.19$ milliseconds for the signal in Figure 7).

The direct implication of the results is that the WWOST could potentially be used for the knock pressure signal analysis. A major advantage of such an approach in comparison to some existing methods is that the signals could be modeled based on a single observation, instead of multiple

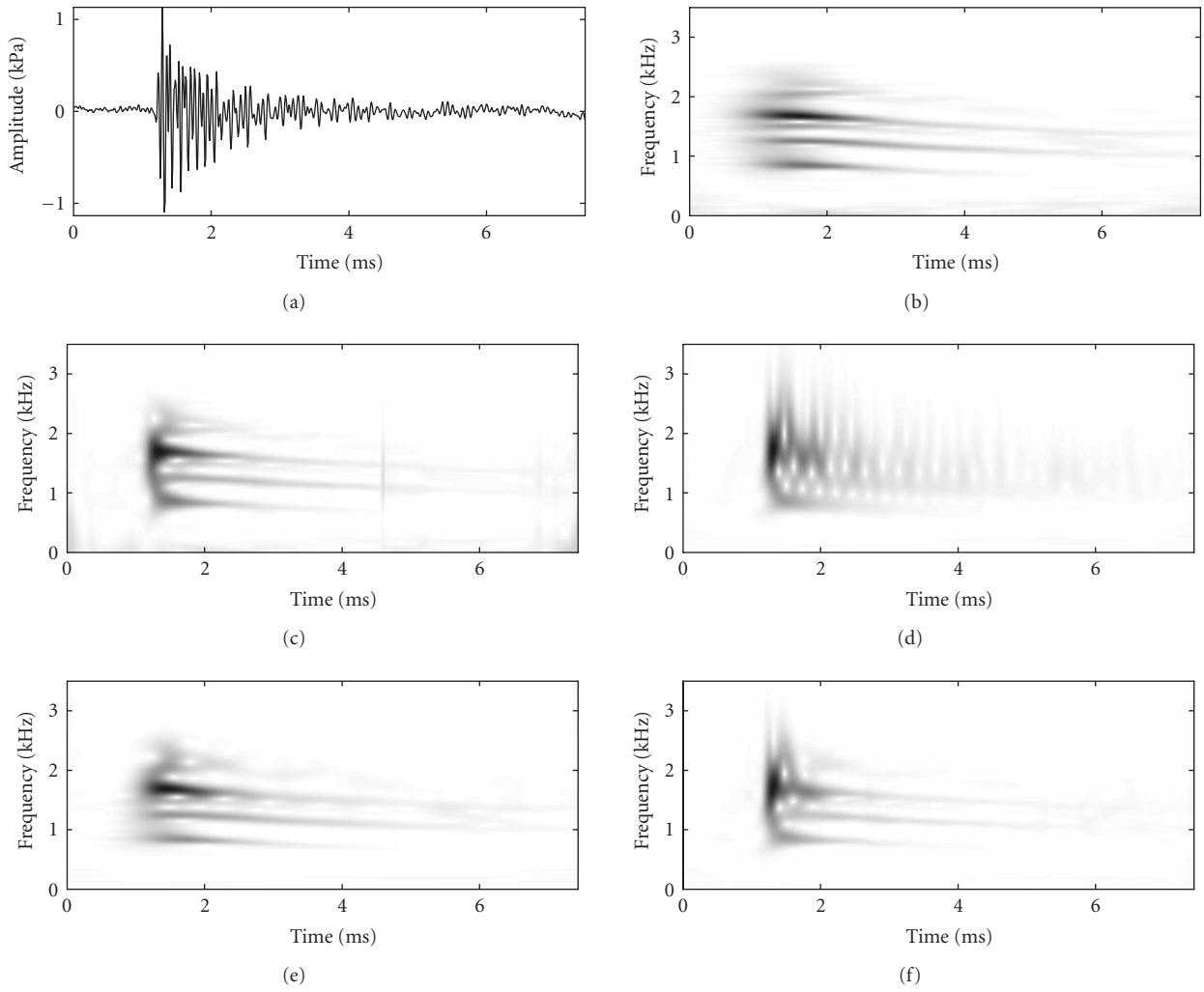


Figure 7: Time-frequency analysis of engine knock pressure signal (48th trial): (a) time-domain representation; (b) STFT; (c) ASTFT with $\sigma_{\text{opt}}(t)$; (d) $S_x^p(t, f)$ with $p = 1$ (standard S-transform); (e) $S_x^p(t, f)$ with $p = 0.87$; (f) $S_x^p(t, f)$ with the optimal $p(t)$.

Table 4: Concentration measures for the two sample trials.

| Trial | $\Xi_{\text{STFT}}$ | $\Xi_{\text{ASTFT}\sigma_{\text{opt}}}$ | $\Xi_{\text{ASTFT}\sigma_{\text{opt}}(t)}$ | $\Xi_{p=1}$ | $\Xi_{p_{\text{opt}}}$ | $\Xi_{p_{\text{opt}}(t)}$ |
|---|---|---|---|---|---|---|
| 17th trial | 0.0057 | 0.0059 | 0.0068 | 0.0054 | 0.0065 | 0.0074 |
| 48th trial | 0.0052 | 0.0054 | 0.0060 | 0.0053 | 0.0058 | 0.0069 |

realizations required by some other time-frequency methods such as Wigner-Ville distribution [23], since the WWOST does not suffer from the cross-terms present in bilinear transforms.

### 4.3. Remarks

It should be noted that, in some cases, when implementing the proposed algorithm, it may be beneficial to window the signal before evaluating $S_x^p(t, f)$ in step (1). This additional step diminishes the effects of a discrete implementation. As shown in [24], wideband signals might lead to some irregular results unless they are properly windowed.

The STFT and the ASTFT are valuable signal decomposition-based representations, which can achieve good energy concentration for a wide variety of signals. However, throughout this paper, it is shown that the proposed optimization of the window width used in the S-transform is beneficial, and in presented cases, it outperforms other standard linear techniques, such as the STFT and the ASTFT. It is also crucial to mention that the WWOST is designed to achieve better concentration in the class of the time-frequency representations based on the signal decomposition.

In comparison to the standard S-transform or the STFT, the WWOST does have a higher computational complexity. The algorithm for the WWOST is based on an optimization procedure and requires a parameter tuning. However, when compared to the transforms of similar group algorithms (e.g., ASTFT), the WWOST has almost the same degree of complexity.

The sampled data version of the standard S-transform and their MATLAB implementations have been discussed in

several publications [5, 7, 25–27]. The WWOST is a straightforward extension of the standard S-transform. Therefore, the sampled data version of the WWOST also follows the steps presented in earlier publications.

## 5. CONCLUSION

In this paper, a scheme for improvement of the energy concentration of the S-transform has been developed. The scheme is based on the optimization of the width of the window used in the transform. The optimization is carried out by means of a newly introduced parameter. Therefore, the developed technique is referred to as a window width optimized S-transform (WWOST). Two algorithms for parameter optimization have been developed: one for finding an optimal constant value of the parameter $p$ for the entire signal; while the other is to find a time-varying parameter. The proposed scheme is evaluated and compared with the standard S-transform by using a set of synthetic test signals. The results have shown that the WWOST can achieve better energy concentration in comparison with the standard S-transform. As demonstrated, the WWOST is capable of achieving higher concentration than other standard linear methods, such as the STFT and its adaptive form. Furthermore, the proposed technique has also been applied to engine knock pressure signal analysis, and the results have indicated that the proposed technique provides a consistent improvement over the standard S-transform.

## ACKNOWLEDGMENTS

Ervin Sejdić and Jin Jiang would like to thank the Natural Sciences and Engineering Research Council of Canada (NSERC) for financially supporting this work.

## REFERENCES

[1] L. Cohen, *Time-Frequency Analysis*, Prentice Hall PTR, Englewood Cliffs, NJ, USA, 1995.

[2] S. G. Mallat, *A Wavelet Tour of Signal Processing*, Academic Press, San Diego, Calif, USA, 2nd edition, 1999.

[3] K. Gröchenig, *Foundations of Time-Frequency Analysis*, Birkhäuser, Boston, Mass, USA, 2001.

[4] I. Djurović and LJ. Stanković, "A virtual instrument for time-frequency analysis," *IEEE Transactions on Instrumentation and Measurement*, vol. 48, no. 6, pp. 1086–1092, 1999.

[5] R. G. Stockwell, L. Mansinha, and R. P. Lowe, "Localization of the complex spectrum: the S-transform," *IEEE Transactions on Signal Processing*, vol. 44, no. 4, pp. 998–1001, 1996.

[6] S. Theophanis and J. Queen, "Color display of the localized spectrum," *Geophysics*, vol. 65, no. 4, pp. 1330–1340, 2000.

[7] C. R. Pinnegar and L. Mansinha, "The S-transform with windows of arbitrary and varying shape," *Geophysics*, vol. 68, no. 1, pp. 381–385, 2003.

[8] C. R. Pinnegar and L. Mansinha, "The bi-Gaussian S-transform," *SIAM Journal of Scientific Computing*, vol. 24, no. 5, pp. 1678–1692, 2003.

[9] M. Varanini, G. De Paolis, M. Emdin, et al., "Spectral analysis of cardiovascular time series by the S-transform," in *Computers in Cardiology*, pp. 383–386, Lund, Sweden, September 1997.

[10] G. Livanos, N. Ranganathan, and J. Jiang, "Heart sound analysis using the S-transform," in *Computers in Cardiology*, pp. 587–590, Cambridge, Mass, USA, September 2000.

[11] E. Sejdić and J. Jiang, "Comparative study of three time-frequency representations with applications to a novel correlation method," in *Proceedings of the IEEE International Conference on Acoustics, Speech and Signal Processing (ICASSP '04)*, vol. 2, pp. 633–636, Montreal, Quebec, Canada, May 2004.

[12] P. D. McFadden, J. G. Cook, and L. M. Forster, "Decomposition of gear vibration signals by the generalized S-transform," *Mechanical Systems and Signal Processing*, vol. 13, no. 5, pp. 691–707, 1999.

[13] A. G. Rehorn, E. Sejdić, and J. Jiang, "Fault diagnosis in machine tools using selective regional correlation," *Mechanical Systems and Signal Processing*, vol. 20, no. 5, pp. 1221–1238, 2006.

[14] P. K. Dash, B. K. Panigrahi, and G. Panda, "Power quality analysis using S-transform," *IEEE Transactions on Power Delivery*, vol. 18, no. 2, pp. 406–411, 2003.

[15] E. Sejdić and J. Jiang, "Selective regional correlation for pattern recognition," *IEEE Transactions on Systems, Man, and Cybernetics, Part A*, vol. 37, no. 1, pp. 82–93, 2007.

[16] LJ. Stanković, "Analysis of some time-frequency and time-scale distributions," *Annales des Telecommunications*, vol. 49, no. 9-10, pp. 505–517, 1994.

[17] LJ. Stanković, "Measure of some time-frequency distributions concentration," *Signal Processing*, vol. 81, no. 3, pp. 621–631, 2001.

[18] D. L. Jones and T. W. Parks, "A high resolution data-adaptive time-frequency representation," *IEEE Transactions on Acoustics, Speech, and Signal Processing*, vol. 38, no. 12, pp. 2127–2135, 1990.

[19] T.-H. Sang and W. J. Williams, "Rényi information and signal-dependent optimal kernel design," in *Proceedings of the 20th IEEE International Conference on Acoustics, Speech and Signal Processing (ICASSP '95)*, vol. 2, pp. 997–1000, Detroit, Mich, USA, May 1995.

[20] W. J. Williams, M. L. Brown, and A. O. Hero III, "Uncertainty, information, and time-frequency distributions," in *Advanced Signal Processing Algorithms, Architectures, and Implementations II*, vol. 1566 of *Proceedings of SPIE*, pp. 144–156, San Diego, Calif, USA, July 1991.

[21] M. Urlaub and J. F. Böhme, "Evaluation of knock begin in spark-ignition engines by least-squares," in *Proceedings of the IEEE International Conference on Acoustics, Speech and Signal Processing (ICASSP '05)*, vol. 5, pp. 681–684, Philadelphia, Pa, USA, March 2005.

[22] I. Djurović, M. Urlaub, LJ. Stanković, and J. F. Böhme, "Estimation of multicomponent signals by using time-frequency representations with application to knock signal analysis," in *Proceediongs of the European Signal Processing Conference (EUSIPCO '04)*, pp. 1785–1788, Vienna, Austria, September 2004.

[23] D. König and J. F. Böhme, "Application of cyclostationary and time-frequency signal analysis to car engine diagnosis," in *Proceedings of IEEE International Conference on Acoustics, Speech, and Signal Processing (ICASSP '94)*, vol. 4, pp. 149–152, Adelaide, SA, Australia, April 1994.

[24] F. Gini and G. B. Giannakis, "Hybrid FM-polynomial phase signal modeling: parameter estimation and Cramér-Rao bounds," *IEEE Transactions on Signal Processing*, vol. 47, no. 2, pp. 363–377, 1999.

[25] R. G. Stockwell, *S-transform analysis of gravity wave activity from a small scale network of airglow imagers*, Ph.D. dissertation, The University of Western Ontario, London, Ontario, Canada, 1999.

[26] C. R. Pinnegar and L. Mansinha, "Time-local Fourier analysis with a scalable, phase-modulated analyzing function: the S-transform with a complex window," *Signal Processing*, vol. 84, no. 7, pp. 1167–1176, 2004.

[27] C. R. Pinnegar, "Time-frequency and time-time filtering with the S-transform and TT-transform," *Digital Signal Processing*, vol. 15, no. 6, pp. 604–620, 2005.